SPATIAL DISTRIBUTION AND CHANGE IN THE SURFACE ICE-VELOCITY FIELD OF VESTFONNA ICE CAP, NORDAUSTLANDET, SVALBARD, 1995–2010 USING GEODETIC AND SATELLITE INTERFEROMETRY DATA

BY
VEIJO A. POHJOLA[1], POUL CHRISTOFFERSEN[2], LESZEK KOLONDRA[3], JOHN C. MOORE[1,4,5], RICKARD PETTERSSON[1], MARTINA SCHÄFER[4], TAZIO STROZZI[6] AND CARLEEN H. REIJMER[7]

[1]Department of Earth Sciences, Uppsala University, Uppsala, Sweden
[2]Scott Polar Research Institute, University of Cambridge, Cambridge, UK
[3]Faculty of Earth Science, University of Silesia, Katowice, Poland
[4]Arctic Centre, University of Lapland, Rovaniemi, Finland
[5]College of Global Change and Earth System Science, Beijing Normal University, 13 Beijing, China
[6]Gamma Remote Sensing and Consulting AG, Gümligen, Switzerland
[7]Institute for Marine and Atmospheric Research, Utrecht University, Netherlands

Pohjola, V.A., Christoffersen, P., Kolondra, L., Moore, J.C., Pettersson, R.S., Schäfer, M., Strozzi, T. and Reijmer, C.H., 2011. Spatial distribution and change in the surface ice-velocity field of Vestfonna ice cap, Nordaustlandet, Svalbard, 1995–2010 using geodetic and satellite interferometry data. *Geografiska Annaler: Series A, Physical Geography*. 93, 323–335. DOI: 10.1111/j.1468-0459.2011.00441.x

ABSTRACT. During 2007 we launched a geodetic campaign on the Svalbard ice cap Vestfonna in order to estimate the velocity field of the ice cap. This was done within the frame of the IPY project KINNVIKA. We present here the velocity measurements derived from our campaigns 2007–2010 and compare the geodetic measurements against InSAR velocity fields from satellite platforms from 1995/96 and 2008. We find the spatial distribution of ice speeds from the InSAR is in good agreement within the uncertainty limits with our geodetic measurements. We observe no clear indication of seasonal ice speed differences, but we find a speed-up of the outlet glacier Franklinbreen between the InSAR campaigns, and speculate the outlet is having a surge phase.

Key words: Arctic ice cap, Austfonna, GPS, ice speed, InSAR, outlet glacier, surge

Introduction

The rapid increase of surface air temperatures in several regions of the High Arctic during the last decade, and the projected increase of Arctic temperatures in the future is prompting close attention to the stability of the Arctic ice caps. While much of the focus has been on the Greenland ice sheet (e.g. Rignot and Kanagaratnam 2006), mountain glaciers and ice caps in the Arctic are at present, and will over the present century, be a large source of eustatic sea level change (Radic and Hock 2011).

One of the large issues at present is to improve the knowledge of how the dynamics of ice masses may change due to warming. Basal lubrication from penetration of surface meltwater to the bed is known to temporarily accelerate the flow of ice along the terrestrial margin of the Greenland ice sheet (Zwally *et al*. 2002; van de Wal *et al*. 2008; Phillips *et al*. 2010) and the mechanism is also observed on Arctic ice caps (Boon and Sharp 2003; den Ouden *et al*. 2010). Marine-terminating outlet glaciers in ice caps and ice sheets also respond similarly in that they are modulating ocean currents and water mass properties in addition to the atmospheric forcing (Holland *et al*. 2008).

To fully understand contemporary cryospheric change, we need observations from a large sample of ice masses, small as well as large, and situated in various settings. Local regimes likely produce a large variability of how the physical processes of glacial flow are affected. For example, the island Nordaustlandet, Svalbard features two large ice caps side-by-side, Austfonna (8120 km^2) and Vestfonna (2402 km^2; Fig 1). The mass balance of these two ice caps is seemingly out of phase with each other. Dowdeswell *et al*. (2008) reported a close to zero mass balance for Austfonna over the past

DOI: 10.1111/j.1468-0459.2011.00441.x

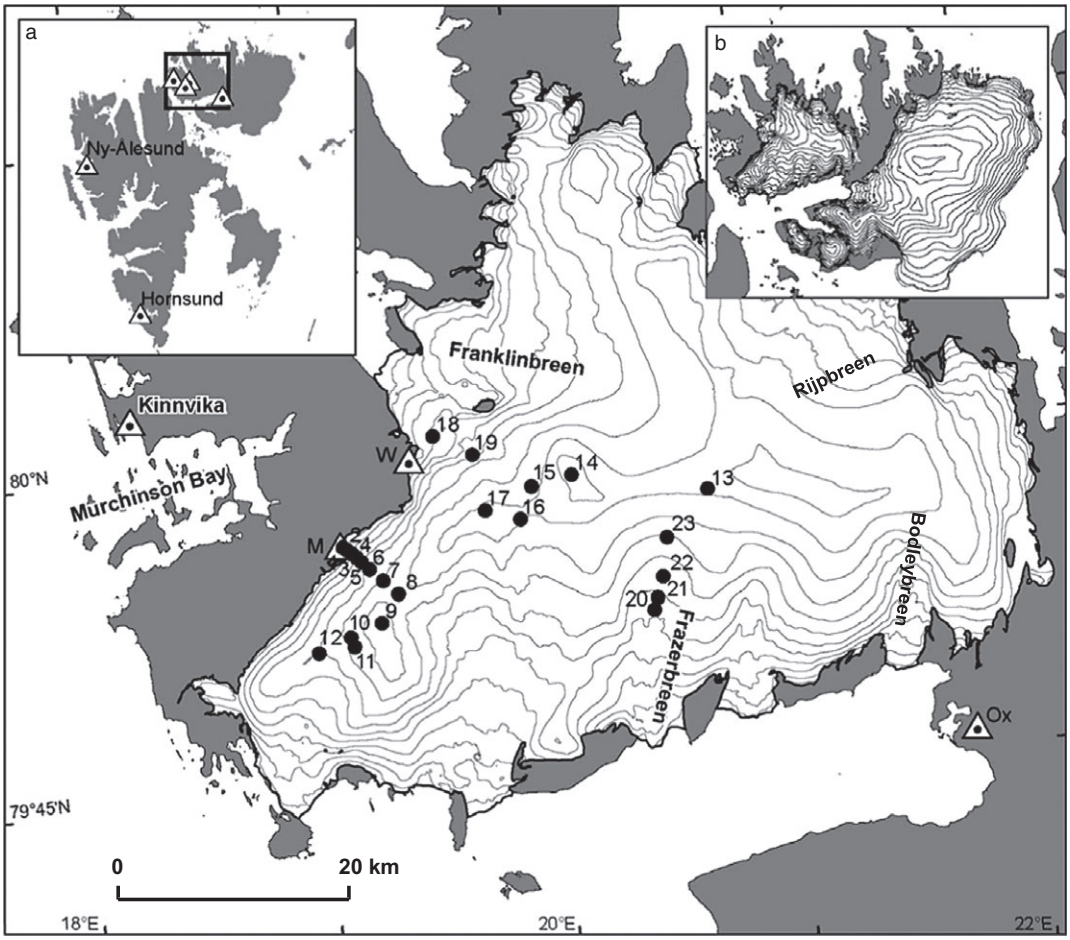

Fig. 1. Svalbard, Nordaustlandet and the ice cap Vestfonna. Elevation- and coast line contours are from the Norwegian Polar Institute DEM. The elevation contour spacing is 500 m. The black dots mark the position markers used for our DGPS surveys. The triangular symbols are the fixed points/base stations (Table 1). The letter at each fixed point/base station refers to the first letter of its name. The Matti and Weasel lobes are the bulging features with fronts ending at the base stations marked with M and W respectively. Donckerfjellet is the terrain SW of Franklinbreen, where the Weasel base station is marked. Inset a) show the base stations and inset b) show the topography of all the ice caps on Nordaustlandet.

decade, but due to calving loss the reported overall balance is negative. Nuth *et al*. (2010) reports an indication of positive balance on Vestfonna. For the present decade the balance trends can be viewed as swapped between the ice caps; with a negative balance for Vestfonna, and a tendency of positive for Austfonna (Bamber *et al*. 2004a, 2004b; Moholdt *et al*. 2010).

The interferometric velocity map of both ice caps presented by Bevan *et al*. (2007) showed a larger part is occupied by fast flowing outlet glaciers on Vestfonna than on Austfonna. This is reflected as a rougher surface on Vestfonna as compared to the smoother Austfonna (Fig. 1). The bedrock topography partly explain the position of outlet glaciers, and the difference in surface topography of the two ice caps (Dowdeswell *et al*. 2008; Pettersson *et al*. 2011), but fails to give a complete answer. Difference in ice margin dynamics and englacial hydrology between the two ice caps may be important processes separating their morphological differences. Further, the different trends in the change in surface elevation, reported for these ice caps may be related to dynamics involved with the marine terminating margins of their outlet glaciers. Hence it is important to improve our knowledge of the dynamics of Arctic ice caps, in order to make improved

assessments of their present and future dynamic regimes possible.

Vestfonna was a major target of multi-disciplinary field campaigns launched within the KINNVIKA project during IPY4 (Pohjola *et al*. 2011). The specific aim of this work is to present the surface velocity field of this ice cap as a benchmark dataset and a first step towards an integrated assessment of the flow and mass balance of Vestfonna. Earlier work has presented satellite-derived velocity fields over Vestfonna (Bevan *et al*. 2007; Strozzi *et al*. 2008). These observations have been contradictory, with large differences in the derived ice speeds. No ground truthed measurements have previously been available. We use satellite interferometry to derive 2D velocity-fields of the ice cap for two different time epochs; 1995/96 and 2008, and ground truth the satellite derived ice speed fields with geodetic measurements done during 2007–2010 through the field program within IPY-KINNVIKA. The geodetic measurements were done both as static surveying of stakes and as continuously recording GPS stations. Using this information we present a field of the ice surface speed of Vestfonna, and discuss the preliminary results of the dynamical situation of the ice cap.

Data and methods

Geodetic data

Establishing a fixed point The first step in our geodetic work was to establish the position of a fixed point in the local coordinate system in Kinnvika. The fixed point used was established by the Norwegian Polar Institute (NPI) for geodetic work at Kinnvika in 1971 (Table 1). We resurveyed the fixed point to establish its coordinates with better accuracy using a Leica 1200 DGPS receiver with 250 hours of observations, during 7 sessions (using a sampling rate of 10 seconds) to gather positional data. We use the term DGPS to describe differential carrier phase positioning. All available observations from the period 30 July to 20 August 2007, were used to compute the coordinates of the NPI-1971 fixed point, using baselines to the SOPAC station in Ny Ålesund (NYA-1) and to the station at Hornsund (SVA028). For the adjustments we used Leica Geo Office v.4.0 software. IGS precise orbits and CODE ionosphere models were imported and applied to the computation of the vectors. The L3 iono-free model without fixing ambiguities was used.

The elevation was determined in the ArcGP 2006 geoid model system. The topographic elevation (m a.s.l.) in this area is *c*. 30 m lower than the WGS 84 ellipsoid elevation. Ellipsoidal coordinates were projected to the UTM 33X zone grid. In the final step the positions of the base stations given in Table 1 were computed radially.

Base stations With the aid of our fixed point, we established base stations on bedrock closer to the glacier in order to shorten baselines for our geodetic work (Table 1, Fig. 1). These base stations were installed in front of the Matti Lobe and on Donckerfjellet (Weasel, 2008–2010 in Table 1), beside the Weasel Lobe of Vestfonna (Fig. 1). We changed from Matti to Weasel base due to change in transportation route from Kinnvika to Vestfonna, thus avoiding sea ice crossing. Matti base was determined in 2007 by a baseline integrated over 2.5 hours (sampling rate 1 second). In 2007 we used Javad Legant GPS for the roving work and Topcon HiPerlite for the base station. Weasel base was determined in 2008–2009 by 6 sessions, altogether over 60 hours of observations (at a sampling rate of 5 seconds). In 2008–2010 we used Trimble R7GNSS and Trimble 5600 with Geodetic Zephyr II antennas for both the base station and the roving station. We further used the base station Oxford, for adjustment of the position of our Weasel base (Table 1). The Oxford

Table 1. Base- and fixed point coordinates and metadata. The UTM coordinates are given as reference in 33X. The elevation is given over the reference ellipsoid WGS 84 in EUREF′89.

Name	Northing (m)	Easting (m)	Elevation (m a.s.l.)	Period (year)
Hornsund (SVA028) Fix	8547010.082	513610.038	43.801	2007
Kinnvika NPI 1971 Fix	8889043.905	561924.588	34.258	2007
Kinnvika Base	8889055.001	562105.806	34.635	2007, 2008
Weasel Base	8885843.539	585567.714	228.27	2008–2010
Matti Base	8878532.889	579730.592	143.99	2007
Oxford Base	8863369.932	633732.654	83.39	2010

station is tied to the NPI grid (Trond Eiken, pers. comm. 8 December 2010).

Ice velocity measurements As a part of a mass balance survey programme 35 mass balance stakes (aluminium, 2 m with 2 + 2 m extensions, 55 mm diameter, 5 mm thick, using internal extensional sleeves of steel tubing) were drilled on Vestfonna in 2007 and maintained to 2010 during repeat spring campaigns using snow mobile transports (Fig. 1). The aim was to use the stakes both as mass balance markers (Möller *et al*. 2011), and as markers for measurements of the surface ice velocities in our DGPS campaigns. Unexpectedly high accumulation rates at the central ridges of Vestfonna resulted in a ~50% loss of these stakes.

During each of the spring campaigns (April–May, 2007 to 2010) we surveyed the position markers. During the campaigns we mounted the antennae on the snow mobiles and measured the altimetry of the ice cap running DGPS in kinematic mode between the stations. When reaching a position marker we switched over to static mode. We also used temporary slave base stations positioned on the ice cap in areas of slow ice flow, as we moved over the ice cap to further shorten the base lines.

Continuously recording GPS stations Between May 2008 and May 2009 we launched a programme to retrieve continuous DGPS positioning records from two of the outlet glaciers of Vestfonna; Franklin- and Frazerbreen. We placed six stations on these glaciers, and one base station on Weasel base. All continuous stations (18–23), except 19 and 20 were equipped with Trimble 5600/R7 units and Trimble Geodetic Zephyr II antennae (Fig. 1). The stations were powered with two 80 Ah batteries, 65 W solar panels and wind turbines (Forgen 500). Stations 19 and 20 were deployed with single frequency IMAU GPS units (den Ouden *et al*. 2010). The Trimble stations generally operated only during the period with light (May–October 2008 and March–May 2009), since the wind turbines did not manage to supply enough power during the dark months, probably because of riming. The IMAU stations were in service over the full period.

Processing of the DGPS data The fixed points and the DGPS stations used in this work are shown in Fig. 1. The post processing of baselines between the used base stations, the slave base stations and the positions markers was done with Trimble Business Centre, using the original Trimble format, or RINEX mode for the Javad data. We used precise ephemeris data for the final processing of the coordinates. The coordinates and the calculated velocities are shown in Fig. 2 and Table 2. All coordinates are in UTM 33X and vertical datum is over the reference ellipsoid WGS 84, projected on UTM 33X.

InSAR data

Tandem Phase ERS-1/2 SAR scenes acquired between December 1995 and January 1996 and four ALOS PALSAR scenes acquired between January 2008 and March 2008 were used to calculate the ice surface velocity structure of Vestfonna. The ERS-1/2 SAR data used here were selected from over 40 winter SAR scenes along ascending and descending orbits (Dowdeswell *et al*. 2008). Image pairs with a suitable baseline combination (i.e., ~60 m for topography and ~30 m for displacement) were preferred. A combination of four-pass differential interferometry (DInSAR) and offset-tracking (Strozzi *et al*. 2002) was employed. DInSAR processing yielded a comprehensive map of ice velocities over almost the whole ice cap, excluding the faster flowing features where offset tracking was considered. The error sources of DinSAR are discussed in Murray *et al*. (2003) and in Dowdeswell *et al*. (2008). In most cases errors are assumed to be smaller than about 2 cm day^{-1} (or ~7 m yr^{-1}). Slant-range and azimuth offset estimation errors are generally better than 1/20th of a pixel for ERS-1/2 Tandem data (Strozzi *et al*. 2002). Combining azimuth offset-tracking displacement maps from both ascending and descending ERS satellite data processed at an azimuth pixel spacing of 4 m allows calculation of three-dimensional ice velocity with an expected error of about 100 m yr^{-1}.

Offset fields between pairs of ALOS PALSAR satellite data acquired with 46 day time-interval were also employed for the estimation of glacier motion over Vestfonna. Offset tracking of L-band SAR images is a robust and direct estimation technique of glacier motion (Strozzi *et al*. 2006; Rignot, 2008; Strozzi *et al*. 2008), particularly useful when DinSAR is limited by loss of coherence due to large acquisition time intervals. Slant-range and azimuth offset estimation errors of ALOS PALSAR data are on the order of 1/10th of a pixel after filtering of occasional azimuth streaks

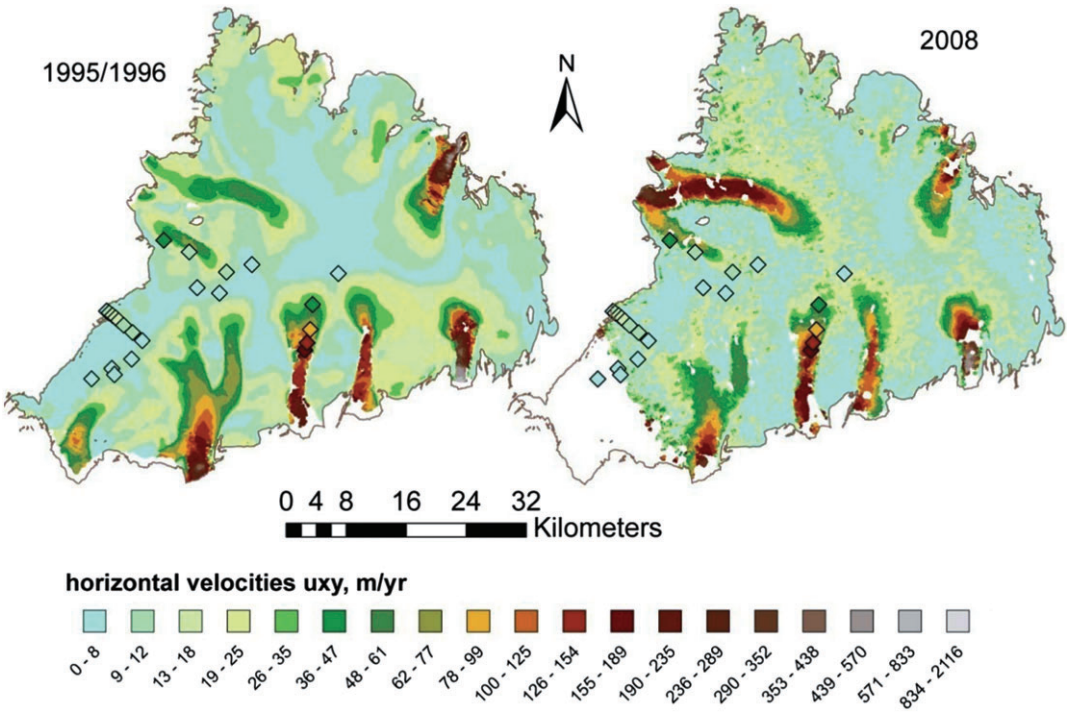

Fig. 2. Vestfonna interferometry speeds during the winters 1995/96 and 2008. The diamonds mark the geodetic measurements at the DGPS stations. Note the fill colour of the diamonds show geodetic speeds, which brings different colours when ice speed from the two methods fall into different classes. The ID of the geodetic (DGPS) positions is found in Fig. 1. The classes are not equally spaced. The southwest area of Vestfonna marked white has no data.

related to auroral zone ionospheric disturbances. For a ground-range pixel spacing of about 7.5 m and an azimuth pixel spacing of about 3 m two-dimensional ice velocity can be computed with an expected error of about 0.8 m in 46 days or better than 10 m yr^{-1} (Rignot and Kanagaratnam 2006). Winter ALOS PALSAR data acquired from 1 February to 18 March 2008, yielded a comprehensive map of ice velocities over large parts of the cap.

The displacement maps derived from satellite SAR data were geocoded to UTM projection at 100 m posting with use of the Norwegian Polar Institute (NPI) DEM. Direct ERS InSAR measurements are along the slant-range direction with an incidence angle of about 23°. Direct ERS offset-tracking measurements are along the azimuth direction. ERS-1/2 data acquired along ascending and descending orbits are combined with both InSAR and offset-tracking in order to retrieve displacement on a horizontal plane. L-band offset-tracking direct measurements are along the SAR slant-range and azimuth directions. For ALOS PALSAR observations incidence angles are about 35°. Slant-range and azimuth offsets are then combined in order to retrieve horizontal displacement.

Results

Geodetically determined horizontal ice speeds

The horizontal ice surface velocity component u_{xy} from the geodetic survey campaigns in 2007–2010 are shown in Table 2. In our scheme u_{xy} is simply the change of position in the plane *x*-*y* over the observation time (*c*. year). The u_{xy} we present is the average value of the velocities measured over the three different survey periods. Not all stations were surveyed during the different survey campaigns, specified in the last three columns in Table 2. The error in u_{xy} is the root mean square (RMS) of the accuracy of the determination of the baseline for each consecutive year in the period. The size of these errors usually reflects the length of the baseline, but is also related to satellite configuration and ionospheric effects. 'Range u_{xy}' is the range between

Table 2. Coordinates of fixed stations and horizontal component u_{xy} of ice surface velocities from geodetic measurements. The elevation is given over the reference ellipsoid WGS 84 in EUREF'89. The error is the RMS of the uncertainty of the baselines to the reference station both years. Range is the difference (u_{xy} max – u_{xy} min) for each station. Ratio is the fraction of the range of total value of u_{xy}. The three last columns show over which period(s) the stations are covered. S denotes static stations, and C continuous stations.

ID	N (m) UTM 33X	E (m) UTM 33X	Elevation (m) WGS84	u_{xy} (m yr^{-1}) average	Error u_{xy} (m) average	Range u_{xy} (m)	Ratio u_{xy}	2007–2008	2008–2009	2009–2010
1	8878333	580087	184	3.18	0.02	0.29	0.09	S	S	S
2	8878110	580418	226	10.57	0.03	0.34	0.03	S	S	S
3	8877769	580873	282	13.38	0.02	0.62	0.05	S	S	S
4	8877452	581257	336	13.43	0.02	0.22	0.02	S	S	S
5	8877074	581681	377	13.26	0.01	0.42	0.03	S	S	S
6	8876463	582346	435	11.81	0.02	0.43	0.04	S	S	S
7	8875493	583523	480	8.13	0.03			S		
8	8874391	584813	512	0.35	0.03			S		
9	8871925	583411	555	0.20	0.03	0.13	0.61	S	S	
10	8870713	580787	498	3.88	0.03			S		
11	8869912	581115	499	5.15	0.04			S		
12	8869372	578072	429	0.44	0.03	0.09	0.21	S	S	
13	8883337	610981	589	7.36	0.03				S	
14	8884515	599450	634	0.59	0.02			S		
15	8883535	596070	564	10.24	0.02				S	
16	8880727	595132	582	1.91	0.03				S	
17	8881461	592143	600	2.68	0.03				S	
18	8887783	587693	267	35.51	0.03				C	
19	8886208	591081	399	8.6	1.4[1]				C	
20	8873106	606508	344	159.5	1.4[1]				C	
21	8874112	606785	375	139.36	0.05				C	
22	8875896	607229	411	84.11	0.05				C	
23	8879203	607538	485	40.11	0.05				C	

[1] The standard deviation of the IMAU GPS at Weasel base May 2009–May 2010.

maximum and minimum u_{xy} over the three possible periods (2007–2008, 2008–2009, 2009–2010). 'Ratio' is the fraction of the total value of u_{xy} divided with 'Range u_{xy}'. Missing values in the 'Range' and 'Ratio' columns correspond to data measured for one period only. The summed errors in the estimation of u_{xy} are 2–3 orders of magnitude smaller than the absolute values of the measured ice speeds, but the range of ice speed between the years is larger. Only 8 of the 23 positions had repeated periods of measurements. Of these 8 stations, the average ratio was 14%, with a maximum ratio of 61%. A part of the annual range is possibly due to dynamical variability in the ice flow. A likely source of this range is due to artefacts in ice motion due to stochastic movement of the position marker in respect to the ice surface (most likely by tilting of the position marker, forced by riming). Note that the ratios higher than 10% correspond exactly to the positions where u_{xy} is smaller than 1 m yr^{-1}.

Spatial distribution of horizontal ice speeds

The satellite derived velocity fields are presented in Fig. 2, where InSAR uxy is parallel to the glacier surface. There is a clear general pattern of slow ice flow on the main area of the ice cap, with pronounced high velocity lanes within the outlet glaciers. Both of the InSAR derived ice velocity scenes show the same general pattern. Fig. 3 shows the ratio and the difference in u_{xy} of the two InSAR scenes of 1995–96 and 2008. Fig. 3a shows a relatively large extent of differing u_{xy} between the two periods. Most of this uncertainty is over the slow flowing area of the ice cap, where the uncertainty of the method is about as large as the derived signal. The maximal uncertainty of the two maps in Fig. 3 is $\pm$ 17 m yr^{-1}, and is in the range of the ice speed outside the outlet glaciers. It is striking that the misfit drastically decreases to a few percent in most of the basins of the fast flowing outlet glaciers. Fig. 3b showing the absolute difference in u_{xy} between the scenes makes a clearer picture of the change in ice speeds on the outlets. The outlets Bodleybreen, Franklinbreen and Rijpbreen all show significant change in speed. The largest difference accounted for is found at Franklinbreen showing at least 2 to 4 times speed-up in the later scene. The northern trunk of Franklinbreen was

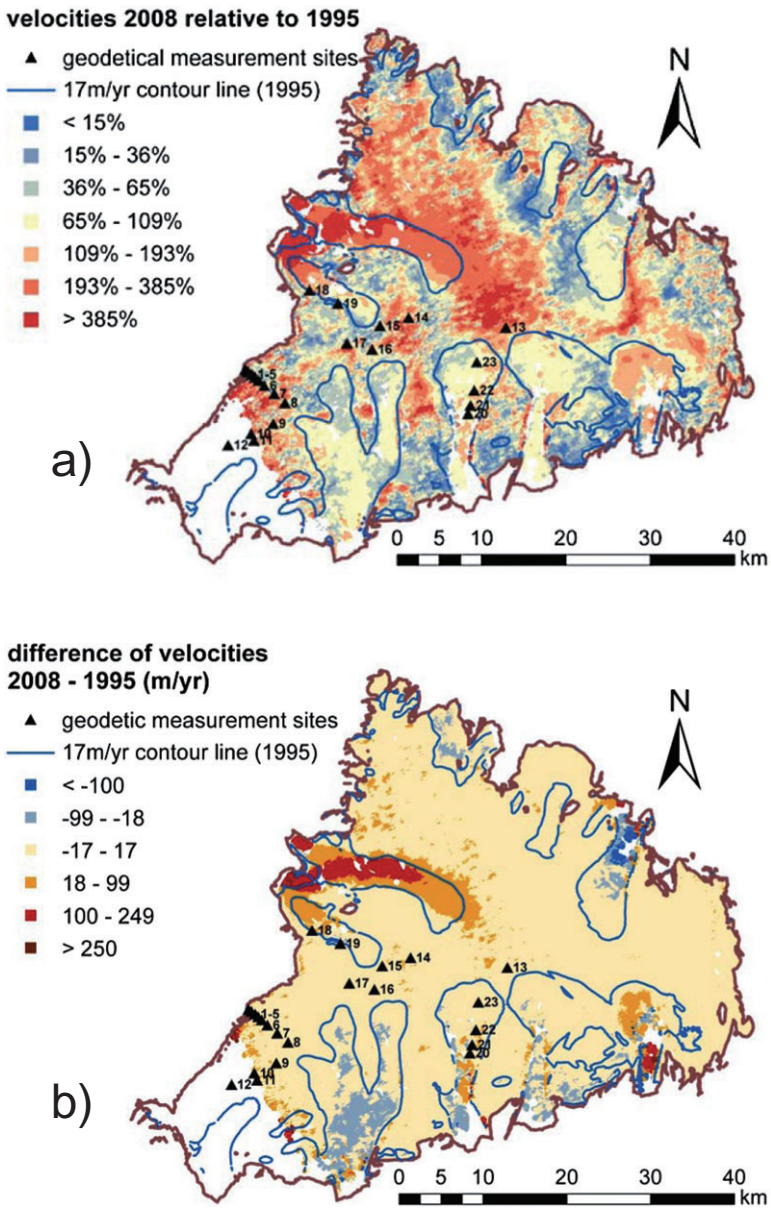

Fig. 3. a) The ratio and b) the difference of InSAR ice speed between the two scenes (2008–1995/96). The 17 m yr^{-1} contour line marks the maximum uncertainty combining the two scenes. The triangles mark the geodetic (DGPS) stations.

reported to have a frontal forward adjustment of ~1 km between 1990 and 2000, and it has been discussed whether this adjustment could have been a result of a surge event (Sneed 2007). Braun *et al.* (2011) report that the advance of the northern trunk of Franklinbreen continued during the last decade, and that the southern trunk of Franklinbreen accompanied the advance. Fig. 3 in conjunction with the results by Braun *et al.* (2011) suggests a surge-like event as a likely explanation of the large difference in u_{xy} we observe between 1994 and 2008.

The speed-up of Bodleybreen may be associated with the minor advance recorded by Braun *et al.*

Table 3. Comparison of ice speeds from geodetic measurements (DGPS) and from the two InSAR periods 1995/96 and 2008. The difference between geodetic data and InSAR is given in separate columns for the two InSAR periods. Bold numbers indicate where the ice speed difference is higher than the uncertainty of the InSAR method. Uncertainty is the combined uncertainty for both the geodetical and the InSAR metods, truncated into m yr^{-1}.

ID	u_{xy} DGPS (m yr^{-1}) average	u_{xy} InSAR 96/96 (m yr^{-1})	Uncertainty (m yr^{-1})	DGPS–InSAR	u_{xy} InSAR 2008 (m yr^{-1})	Uncertainty (m yr^{-1})	DGPS–InSAR
1	3.18	5.33	7	2.15	4.49	10	1.31
2	10.57	7.57	7	–3.00	9.18	10	–1.39
3	13.38	9.74	7	–3.64	11.34	10	–2.04
4	13.43	9.69	7	–3.74	7.57	10	–5.86
5	13.26	9.82	7	–3.44	4.66	10	–8.60
6	11.81	9.12	7	–2.69	7.40	10	–4.41
7	8.13	6.68	7	–1.45	3.05	10	–5.08
8	0.35	6.41	7	6.06	8.66	10	8.31
9	0.20	8.49	7	**8.29**	18.26	10	**18.06**
10	3.88	9.87	7	5.99	25.38	10	**21.50**
11	5.15	9.71	7	4.56	28.00	10	**22.85**
12	0.44	6.10	7	5.66			
13	7.36	5.97	7	–1.39	18.85	10	**11.49**
14	0.59	7.11	7	6.52	6.39	10	5.80
15	10.24	12.99	7	2.75	11.58	10	1.34
16	1.91	7.85	7	5.94	12.05	10	**10.14**
17	2.68	6.44	7	3.76	2.78	10	0.10
18	35.51	19.28	7	**–16.23**	53.19	10	**17.68**
19	8.6	17.49	8	**8.9**	8.25	11	–0.3
20	159.5	147.78	8	**–11.7**	138.50	11	**–21.0**
21	139.36	139.29	7	–0.07	129.90	10	–9.46
22	84.11	86.75	7	2.64	77.98	10	–6.13
23	40.11	45.30	7	5.19	37.24	10	–2.87

(2011) between 1984 and 2000. The slow-down of Rijpbreen may be associated with the retreat of that outlet (Braun *et al*. 2011). We have no control point on either Bodleybreen or Rijpbreen, and both these outlets had a fragmentary coverage in the 2008 scene, so we leave the speed change on these outlets out in the coming discussion. Excluding these three outlets, we find the two InSAR spatial distribution of u_{xy} on Vestfonna are similar to each other more or less within the uncertainty of the method.

Comparing horizontal ice speeds derived from the two methods

In Table 3 and Fig. 4 we compare the geodetic u_{xy} with u_{xy} from InSAR. We find that the difference in the ice speeds derived from the two different sources in most cases is less than the uncertainty of the least accurate method. The uncertainty of the InSAR method is generally more than an order of magnitude larger than the geodetic measurements, leading to the fact that the uncertainty in the InSAR data governs the combined uncertainty of the geodetic and the InSAR data. Eleven of the 45 common points for 1995/96 and 2008 have a difference larger than the uncertainty limits. Seven of these points are in the 2008 InSAR scene, and may suggest that this scene is less reliable than the 1995/96 scene. This is confirmed by the more broken up pattern in the 2008 scene, as compared to the 1995/96 scene (Fig. 2). The reason for the difference is that in 2008 we used offset tracking, due to low coherence. This produced larger uncertainties than in the 1995/96 scene. The difference between geodetic and InSAR velocities in points 10, 11, 13 and 16 may be explained by the lower coherence in the 2008 data. Note that these points are close to the limits of uncertainty (13, 16) and data coverage (10, 11).

The four points having a difference between geodetic and InSAR 1995/96 velocities larger than the uncertainty level, are points 9, 18, 19 and 20 (Table 3). All these points except point 19 show a substantial difference between geodetic and InSAR 2008 velocities. Point 9 has a geodetic $u_{xy} < 1$ m yr^{-1}, and this may be a reason of the misfit. Points 18 and 19 are situated on the southern

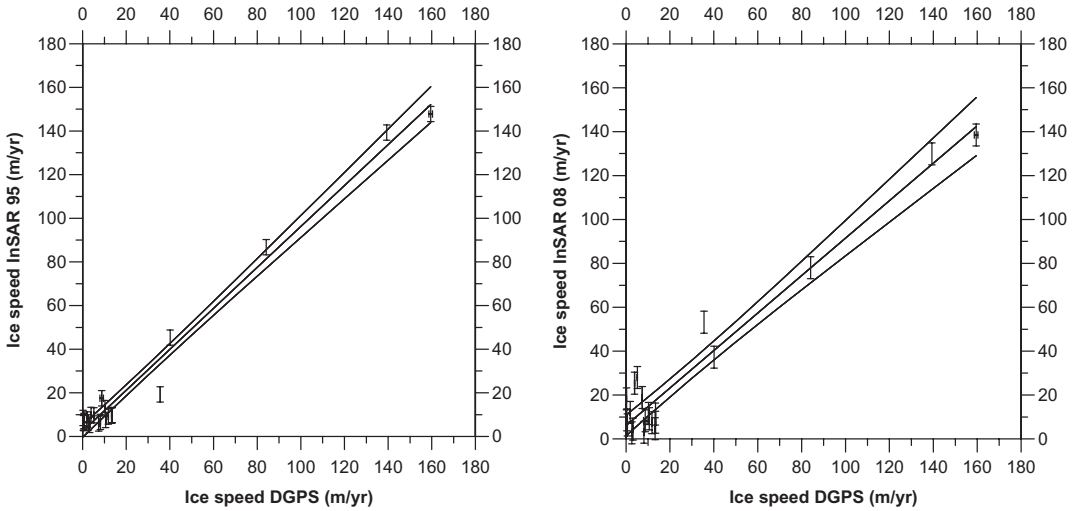

Fig. 4. Comparison of InSAR and geodetical (DGPS) ice speeds, a) shows InSAR 1995/96 and b) InSAR (2008). The error bars are from Table 2 (DGPS) and Table 3 (InSAR). Note that the InSAR uncertainty is more than a magnitude larger than DGPS uncertainty in most cases. The linear regressions (inner lines) are $r^2 = 0.96$ (a) and $r^2 = 0.89$ (b). The outer lines show the 95% confidence intervals.

trunk of Franklinbreen that advanced from 2000 and onwards (Braun *et al*. 2011). The factor of 1.5 increases in InSAR u_{xy} between 1994 and 2008 for point 18 may be an acceleration reflecting that effect, and explain the overall misfit between the different temporal ice speed measurements. Worth to note is that points 19 and 20 were measured with single phase GPSs, with a lower accuracy than the DGPS stations (Table 2) and may explain a part of the difference between the geodetic and InSAR ice speeds.

The other outlet glacier from which we have geodetic control points, Frazerbreen, show no deviation on geodetic and InSAR u_{xy} within the uncertainty limits, with one exception. Point 20 shows a lower InSAR to geodetic u_{xy} for both scenes. This may be related to the lower accuracy of the GPS used here, as described above. Fig. 4 shows the linear regression between the InSAR and geodetic u_{xy}, and illustrates the generally good fit within the uncertainty of the InSAR method between the InSAR and geodetically derived u_{xy} of Vestfonna.

Discussion

We find the spatial distribution of the horizontal ice velocity u_{xy} from the InSAR scenes are within the uncertainty limits of the geodetic u_{xy} at the control points. This is a good affirmation of the InSAR methods we used. Bevan *et al*. (2007) published InSAR ice speed field over Vestfonna using single-track ERS-1 imagery from 1994, but their speeds were a factor of 0.2–0.5 smaller than the ice speeds we derived from the 1995/96 scenes. Repeating our InSAR for another period (2008), and adding the ground-truthing from geodetic measurements over the same period corroborates the ice speed field from our results. These results will be used in our forthcoming ice flow model experiments; efforts we are pursuing in order to better understand the dynamics of Vestfonna.

One issue to consider is how comparable the InSAR and geodetic u_{xy} in reality are. The InSAR u_{xy} is based on images covering periods of around 50 days while the geodetic measurements cover periods of nearly a year. This can potentially lead to two different effects; 1) The longer measurement period for the geodetic surveys leads to an integration of ice speed variations over the distance that the stake moves over this period and; 2) Temporal variations in the ice speed influence the geodetic measurements due to the long measuring period. In the first case, the geodetic method could be considered as a Lagrangian measurement, while the InSAR method can be regarded to be more like a true Cartesian system. Normally the effect of assuming a Cartesian system within a system in motion would have little error if the average u_{xy} is small. In our data the points 20 and 21 have the highest values of u_{xy} and can be used to estimate the maximal 'Lagrangian' effect on our geodetic u_{xy}.

Between point 20 and 21 we have a strain rate of ~0.07 yr^{-1} (the difference in speed between point 20 and 21 (20.1 m yr^{-1})/distance between the points (277 m)). If we assume a constant strain rate, then u_{xy} at point 21 during a year is likely given by $u_{xy} = 139 - (139 \times 0.07 / 2) = 134$ m yr^{-1}. The difference of about 5 m yr^{-1} is smaller than the uncertainty in the InSAR method, and does not induce larger uncertainties in our work.

Regarding the InSAR measurements, they are truer in the Cartesian system in the temporal field than the geodetical measurements, as discussed above. But since the InSAR ice motion is an average of a pixel resampled to 100 × 100 m (from 50 × 50 m 1995/96 and 1 × 1 km 2008) they are spatially averaged, while the geodetic measurements are true point measurements. This introduces another ambiguity in the comparison of the data types we use, and is one of the reasons why the InSAR uncertainties are relatively high.

Another issue to consider is whether Vestfonna outlets experience seasonal velocity variability as has been reported for other outlet glaciers in the Arctic (Joughin *et al*. 2008; van de Wal *et al*. 2008; den Ouden *et al*. 2010). Both InSAR scenes are over winter months, while the geodetic u_{xy} are averaged over the full year (May to May). If Vestfonna outlets experience speed-ups during summer then the InSAR u_{xy} would underestimate the annual u_{xy}. From our continuous DGPS stations we managed to get six records operating over summer and through the following winter months (Table 4). From these six stations, only one station, point 19 on Franklinbreen showed a substantial increase in speed (about a factor of 2 increase) for the summer months compared to the winter months. Notable is that the other station on Franklinbreen, point 18 during the same interval show a 24% decrease in speed during summer as compared to the winter months. None of the Frazerbreen stations show any seasonal differences in average u_{xy}. From this, we regard that seasonal bias can have influence in the comparison on Franklinbreen, but is not likely for the other positions we use.

The discovery of speed-up of Franklinbreen is an interesting result. Sneed (2007) studied frontal adjustments from aerial photographs and from ASTER imagery the years 1966–71, 1990, 2000, 2001, 2005) and found a 1 km frontal advance between 1990 and 2000 of the northern trunk of Franklinbreen. Franklinbreen was reported to have surged in 1956 by Hagen *et al*. (1993), but Sneed (2007) found no morphological evidence of a surge, such as looped moraines, or a heavily crevassed carapace, and doubted that Franklinbreen went through a surge cycle in 1966–2005. In addition the southern trunk of Franklinbreen had a different pattern of frontal adjustment, with a general retreat between 1971 to 2000 of over 1 km, and *c*. 0.5 km frontal advance between 2000 and 2005. The observed difference between advance and retreat of the two trunks may suggest a complex internal dynamics of Franklinbreen, rather than a general surge of the outlet glacier as a whole. Braun *et al*. (2011) show that both trunks of Franklinbreen have advanced over the last decade, which is in agreement with our results showing speed up of both trunks by a factor of >2 between 1994 and 2008. In the upstream accumulation area we only find speed-up on the northern trunk, whereas the upstream area of the southern trunk has remained stable or even slowed down. This may give further evidence of a complex interplay between the two parts of Franklinbreen. Svalbard glaciers are known to have slower, and less pronounced surging behaviour than glaciers in warmer environments (Dowdeswell *et al*. 1991; Murray *et al*. 2003; Sund *et al*. 2009).

Thermal control on the basal properties is likely an important aspect of the fast flow on Vestfonna. The radio-echo soundings by Pettersson *et al*. (2011) show that the slow-moving ridges of Vest-

Table 4. Seasonal variation in ice speed on the outlet glaciers Franklin- and Frazerbreen. JJA is June to August, DJF is December to February. Days indicates how many days of ice velocity data was available within the given time period.

ID	u_{xy} JJA (m yr^{-1})	Interval length (days)	u_{xy} DJF (m yr^{-1})	Interval length (days)	JJA/DJF-ratio
18	30.15	25	39.75	31	0.76
19	14.54	92	6.55	92	2.22
20	150.09	92	164.98	91	0.91
21	141.83	31	142.92	18	0.99
22	88.58	31	87.52	18	1.01
23	42.36	31	41.18	19	1.03

fonna are cold-based. The radio-echo soundings also show that englacial water is available to lubricate the fast flow of the adjacent outlet glaciers. They further show that the outlets are, at least partially, wet based. We speculate that the faster flowing outlets, including Frazerbreen on the southern rim of Vestfonna may be in a continuous high ice-flow mode, while Franklinbreen's two competing branches may have a larger potential to resist the overburden pressure than the outlet glaciers of the southern rim of Vestfonna, explaining the relatively large ice speed differences detected in our study. If this larger potential to resistance is a factor of topography, mass balance or some other internal dynamics is impossible to say, but ongoing modelling of ice dynamics of the ice cap and in particular Franklinbreen may bring an answer in the future. Bodleybreen was reported to surge during the 1970s (Dowdeswell *et al*. 1991). We note that although the surge culminated in the early 1980s, the ice speed is still high, and Bodleybreen may not have as strong switch as Franklinbreen in its surge cycle. Our results suggest that Vestfonna is more strongly influenced by fast glacier flow and thus in a different dynamic state compared to Austfonna. Austfonna has a larger accumulation area, but a smaller fraction of fast flowing outlet glaciers relative to size, and therefore a more even surface than Vestfonna (Dowdeswell *et al*. 2008). This difference in dynamic influence of outlet glaciers may be a part of the reported difference in mass balance states between these two ice caps (Bamber *et al*. 2004a, b; Dowdeswell *et al*. 2008; Nuth *et al*. 2010; Moholdt *et al*. 2010), Vestfonna may be more sensitive to those processes resulting in dynamic thinning along the margin of the Greenland ice sheet due to its larger outlet glacier/ice cap area ratio than Austfonna.

We conclude that our derived InSAR velocity fields compare well with the ground-truthing we have from geodetic measurements of ice speeds. We also find that ice speeds are comparable, within the uncertainty and resolution, between our methods within our different periods of cover. The exception to this is Franklinbreen, where a pronounced speed-up during the last decade is detected. We further suggest that the balance and/or elevation change of Vestfonna may be more controlled by the outlet glaciers dynamics than Austfonna due to Vestonna's larger outlet glacier / ice cap area ratio. We finally hope that with this we have taken a small step forward into providing benchmark information for a better understanding of the dynamics of Vestfonna in particular, and Arctic ice caps in general.

Acknowledgements

Alun Hubbard is acknowledged for his services and input into this project. Without the logistical support of IPY-KINNVIKA we would never had managed this work. Piotr Głowacki's engagement for IPY-KINNVIKA was of paramount importance to us. The logistical support from The Swedish Polar Research Secretariat, The Polish Polar Station, The ship and personnel of *RV Horyzont II* of the Polish Marine Academy, The ship and personnel of the Norwegian coast guard *Svalbard*, UNIS and the Norwegian Polar Institute are acknowledged for excellent support. We further thank Naviga and Airlift A/S for their valuable services. The Governor of Svalbard is to be thanked for giving us permission to use the old IPY-3 station Kinnvika. All hands of IPY-KINNVIKA are thanked for making our common endeavour into such a success. Special thanks to Per-Olof Edvinsson, Janne Johansson, Lasse Tano and Åke Wallin for service in the field, and the field hands by Harvey Goodwin, Ulf Jonsell, Denis Samyn, and Peter Sjögren. Trond Eiken and Jon Ove Hagen are acknowledged for sharing DGPS data and service at the Oxford station. Financial support by The Nordic Council of Ministers and The Swedish Polar Research Secretariat was paramount to IPY-KINNVIKA. VP acknowledges funds from the Swedish Research Council. TS acknowledge the EU Framework 6 Program INTEGRAL Project and from the ESA project GlobGlacier. Further, the InSAR data is acknowledged by (ERS-1/2 SAR data courtesy C1P.2611, © ESA; ALOS PALSAR data courtesy AOPOL.4086, © JAXA; DEM of Nordaustlandet © NPI). We acknowledge SPIRIT-SPOT 5 stereoscopic survey of Polar Ice: Reference Images and Topographies during the fourth International Polar Year (2007–2009) for imagery used for navigation and mapping. Installation of GPS systems on Frazerbreen and Franklinbreen was supported by NERC grant NE/F011466/1 awarded to PC and AH. Finally, we thank the two anonymous reviewers and the editorial skills of Paula Kankaanpää for assistance into the final product. This is SVALI publication no.1 and an ESF-SvalGlac publication.

Veijo A. Pohjola, Department of Earth Sciences, Air, Water and Landscape Science, Uppsala 410 University, Villavägen 16, 752 36 Uppsala, Sweden.
Email: Veijo.pohjola@geo.uu.se

Polu Christoffersen, Scott Polar Research Institute, University of Cambridge, Lensfield Road, 413 Cambridge, CB2 1ER, UK.

Leszek Kolondra, Faculty of Earth Science, University of Silesia, ul. Bankowa 12, Katowice, Poland.

John C. Moore, Department of Earth Sciences, Air, Water and Landscape Science, Uppsala University, Villavägen 16, 752 36 Uppsala, Sweden; Arctic Centre, University of Lapland, POB 122, FI-96101 Rovaniemi, Finland; and College of Global Change and Earth System Science, Beijing Normal University, 19 Xinjiekou Wai Street, 100875, Beijing, China.

Rickard Pettersson, Department of Earth Sciences, Air, Water and Landscape Science, Uppsala 410 University, Villavägen 16, 752 36 Uppsala, Sweden.

Martina Schäfer, Arctic Centre, University of Lapland, POB 122, FI-96101 Rovaniemi, Finland.

Tazio Strozzi, Gamma Remote Sensing and Consulting AG, Worbstrasse 225, 3073 Gümligen (BE), Switzerland.

Carleen H. Reijmer, Institute for Marine and Atmospheric Research, Utrecht University, Princetonplein 5 3584CC, Utrecht, Netherlands.

References

Bamber, J., Krabill, W., Raper, V. and Dowdeswell, J., 2004a. Anomalous recent growth of part of a large Arctic ice cap: Austfonna, Svalbard. *Geophysical Research Letters*, 31, L12402, doi:10.1029/2004GL019667.

Bamber, J.L., Krabill, W., Raper, V., Dowdeswell, J.A. and Oerlemans, J., 2004b. Elevation changes measured on Svalbard glaciers and ice caps from airborne laser data. *Annals of Glaciology*, 42, 202–208.

Bevan, S., Luckman, A., Murray, T., Sykes, H. and Kohler, J., 2007. Positive mass balance during the late 20th century on Austfonna, Svalbard, revealed using satellite radar interferometry. *Annals of Glaciology*, 46, 117–122.

Boon, S. and Sharp, M., 2003. The role of hydrologically-driven ice fracture in drainage system evolution on an Arctic glacier. *Geophysical Research Letters*, 30 (18), 1916, doi:10.1029/2003GL018034.

Braun, M., Pohjola, V.A., Pettersson, R., Möller, M., Finkelnburg, R., Falk, U., Scherer, D., and Schneider, C., 2011. Changes of glacier frontal positions of Vestfonna (Nordaustlandet, Svalbard). *Geografiska Annaler, Series A, Physical Geography*. doi: 10.1111/j.1468-0459.2011.00437.x.

den Ouden, M.A.G., Reijmer, C.H., Pohjola, V., van de Wal, R.S.W., Oerlemans, J. and Boot, W., 2010. Stand-alone single-frequency GPS ice velocity observations on Nordenskiöldbreen, Svalbard. *The Cryosphere*, 4, 593–604, doi:10.5194/tc-4-593-2010.

Dowdeswell, J., Benham, T., Strozzi, T. and Hagen, J., 2008. Iceberg calving flux and mass balance of the Austfonna ice cap on Nordaustlandet, Svalbard. *Journal of Geophysical Research*, 133, F03022, doi:10.1029/2007JF000905.

Dowdeswell, J.A., Hamilton, G.S. and Hagen, J.O., 1991. The duration of the active phase on surge-type glaciers: contrasts between Svalbard and other regions. *Journal of Glaciology*, 37 (127), 388–400.

Hagen, J.O., Liestøl, O., Roland, E. and Jørgensen, T., 1993. *Glacier Atlas of Svalbard and Jan Mayen*. Norsk Polarinstitutt Meddelser 129.

Holland, D.M., Thomas, R.H., De Young, B., Ribergaard, M.H. and Lyberth, B., 2008. Acceleration of Jakobshavn Isbrae triggered by warm subsurface ocean waters. *Nature Geoscience*, 1, 659–664. doi:10.1038/ngeo316

Joughin, I., Das, S.B., King, M.A., Smith, B.E., Howat, I.M. and Moon, T., 2008. Seasonal speed up along the western flank of the Greenland Ice Sheet. *Science*, 320, 781–783, doi:10.1126/science.1153288.

Moholdt, G., Nuth, C., Hagen, J.O. and Kohler, J., 2010. Recent elevation changes of Svalbard glaciers derived from ICESat laser altimetry. *Remote Sensing of the Environment*, 114, 2756–2767.

Möller, M., Möller, R., Beaudon, É., Mattila, O.-P., Finkelnburg, R., Braun, M., Grabiec, M, Jonsell, U., Luks, B., Puczko, D., Scherer, D. and Schneider, C., 2011. Snowpack characteristics of Vestfonna and De Geerfonna (Nordaustlandet, Svalbard) – a spatiotemporal analysis based on multiyear snow-pit data. *Geografiska Annaler, Series A: Physical Geography*. doi: 10.1111/j.1468-0459.2011.00440.x.

Murray, T., Strozzi, T., Luckman, A., Jiskoot, H. and Christiakos, P., 2003. Is there a single surge mechanism? Contrasts in dynamics between glacier surges in Svalbard and other regions. *Journal of Geophysical Research*, 108 (B5), doi:10.1029/2002JB001906.

Nuth, C., Moholdt, G., Kohler, J., Hagen, J.O. and Kääb, A., 2010. Svalbard glacier elevation changes and contribution to sea level rise. *Journal of Geophysical Research*, 115, (F01008), doi:10.1029/2008JF001223.

Pettersson, R., Christoffersen, P., Dowdeswell, J.A., Pohjola, V., Hubbard, A. and Strozzi, T., 2011. Ice thickness and basal conditions of Vestfonna ice cap, eastern Svalbard. *Geografiska Annaler, Series A, Physical Geography*. doi: 10.1111/j.1468-0459.2011.00438.x.

Phillips, T., Rajaram, H. and Steffen, K., 2010. Cryo-hydrologic warming: A potential mechanism for rapid thermal response of ice sheets. *Geophysical Research Letters*, 37 (L20503), doi:10.1029/2010GL044397.

Pohjola, V.A., Kankaanpää, P., Moore, J.C. and Pastusiak, T., 2011. The international polar year project 'KINNVIKA' – Arctic warming and impact research at 80 °N. *Geografiska Annaler, Series A, Physical Geography*. doi: 10.1111/j.1468-0459.2011.00436.x.

Radic, V. and Hock, R., 2011. Regionally differentiated contribution of mountain glaciers and ice caps to future sea-level rise. *Nature Geoscience*, 4, 91–94, doi: 10.1038/ngeo1052.

Rignot, E., 2008. Changes in West Antarctic ice stream dynamics observed with ALOS PALSAR data. *Geophysical Research Letters*, 35(L12505), doi:10.1029/2008GL033365.

Rignot, E. and Kanagaratnam, P., 2006. Changes in the velocity structure of the Greenland ice sheet. *Science*, 311, 986–990, doi: 10.1126/science.1121381.

Sneed, W.A.,jr., 2007. *Satellite remote sensing of Arctic glaciers – climate interactions*. MSc thesis, University of Maine, USA.

Strozzi, T., Kouraev, A., Wiesmann, A., Wegmülle, U., Sharov, A. and Werner, C., 2008. Estimation of Arctic glacier motion with satellite L-band SAR data. *Remote Sensing of Environment*, 112, 636–645.

Strozzi, T., Luckman, A., Murray, T., Wegmüller, U. and Werner, C., 2002. Glacier motion estimation using SAR offset-tracking procedures. *IEEE Transactions on Geoscience and Remote Sensing*, 40 (11), 2384–2391.

Strozzi, T., Weismann, A., Sharov, A., Kouraev, A., Wegmuller, U. and Werner, C., 2006. Capabilities of L-band SAR data for Arctic glacier motion estimation. In: Anonymous (ed). *2006 IEEE International Conference on Geoscience and Remote Sensing Symposium*, 3816–3819, doi: 10.1109/igarss.2006.978.

Sund, M., Eiken, T., Hagen, J.O. and Kääb, A., 2009. Svalbard surge dynamics derived from geometric changes. *Annals of Glaciology*, 50 (52), 50–60.

van de Wal, R.S.W., Boot, W., van den Broeke, M.R., Smeets, C.J.P.P., Reijmer, C.H., Donker, J.J. A. and Oerlemans, J., 2008. Large and rapid melt-induced velocity changes in the ablation zone of the Greenland ice sheet. *Science*, 321, 111–113, doi: 10.1126/science.1158540.

Zwally, H.J., Abdalati, W., Herring, T., Larson, K., Saba, J. and Steffen, K., 2002. Surface melt-induced acceleration of Greenland ice-sheet flow. *Science*, 297, 218–222, doi: 10.1126/science.1072708.

Manuscript received Jan., 2011, revised and accepted Aug., 2011